J Atmos Chem
DOI 10.1007/s10874-006-9048-4

Biogenic Hydrocarbon Chemistry within and Above a Mixed Deciduous Forest

Jose D. Fuentes · Daniel Wang · Dave R. Bowling · Mark Potosnak · Russell K. Monson · Wendy S. Goliff · William R. Stockwell

Received: 25 May 2006 / Accepted: 18 September 2006

Abstract This manuscript includes findings from field and numerical modeling investigations designed to quantify the degree and rates of biogenic hydrocarbon chemical processing within and above a mixed deciduous forest in the southeastern United States. The study site was under the influences of nitrogen oxide and hydrocarbon emissions from suburban automobile traffic. The most common ambient biogenic hydrocarbons measured within and above the forest included isoprene, α-pinene, and d-limonene. Isoprene was the most abundantly produced biogenic hydrocarbon, with maximum isoprene flux densities reaching 50 nmol m^{-2} s^{-1}. Isoprene and its reaction products (methyl vinyl ketone and methacrolein) comprised over 75% of the measured hydrocarbon mass. Substantial nitrate (NO_3) and hydroxyl (HO) radical formation occurred within the forest canopy, with maximum NO_3 and HO levels approaching 1 part per trillion on a volume basis (pptv) and

J. D. Fuentes (✉)
Department of Environmental Sciences, University of Virginia,
Clark Hall, 291 McCormick Road, Charlottesville, VA 22904, USA
e-mail: jf6s@virginia.edu

D. Wang
Environmental Technology Center, Environment Canada,
335 River Road South, Ottawa, ON K1A 0H3, Canada

D. R. Bowling
Department of Biology, University of Utah, Salt Lake City, UT 84112, USA

M. Potosnak
Division of Earth and Environmental Sciences, Desert Research Institute, Reno, NV 89512, USA

R. K. Monson
Department of Ecology and Evolutionary Biology, and Cooperative Institute for Research
in Environmental Sciences, University of Colorado, Boulder, CO 80309, USA

W. S. Goliff
Division of Atmospheric Sciences, Desert Research Institute, Reno, NV 89512, USA

W. R. Stockwell
Department of Chemistry, Howard University, Washington, DC 20059, USA

0.05 pptv, respectively. These NO_3 and HO levels, combined with within-canopy ozone (O_3) mixing ratios of 60 parts per billion (ppbv), reacted with biogenic hydrocarbons and produced substantial amounts (0.6 ppbv) of peroxy radicals. The main conclusion from this investigation is that forested ecosystems capable of high rates (>50 nmol m^{-2} s^{-1}) of biogenic hydrocarbon emissions, and in the vicinity of modest rates of nitrogen oxide emissions from suburban automobile traffic, can support a unique and active photochemistry within the forest canopy. In these areas it may not be valid to use biogenic emissions estimated from measurements made at the foliage level for regional-scale air quality modeling because the underlying processes are nonlinear. Regional-scale air quality models should include chemical preprocessing of biogenic hydrocarbons before they are emitted to the full regional modeling grid in order to accurately represent the photochemical production of pollutants on the wider scale.

Key words air pollution · biogenic hydrocarbons · hydroxyl radicals · isoprene · peroxy radicals · oxidants

1 Introduction

In eastern North America forest coverage is approaching the levels experienced during pre-colonial times (Fitzjarrald et al., 2001; Foster, 1992). The emerging dominant plant species include oaks (*Quercus alba L.*), tulip poplar (*Liriodendron tulipifera* L.), sweet gum (*Liquidambar styraciflua*), red maple (*Acer rubrum*), and loblolly pine (*Pinus taeda* L.) (Orwig and Abrams, 1994). These tree species are known to be among the most effective biogenic hydrocarbon emitters (Geron et al., 2000). In addition, eastern North American forests ordinarily develop vegetated canopies often reaching 20 m in height, with leaf area indices (LAI = ratio of planar leaf area to ground area) ranging from 2 to 6. For sparse forest canopies, whose LAI is less than 3, substantial actinic fluxes can reach the lower depths of the canopy to promote photochemical reactions. In the case of tall and dense forests, canopy architecture and associated levels of atmospheric turbulence govern the characteristic within-canopy air parcel residence times which can reach tens of minutes (Strong et al., 2004). These time scales are comparable to or greater than the lifetimes of biogenic hydrocarbons such as β-caryophyllene (Fuentes et al., 2000; Jaoui et al., 2003). Because of the abundance of oxidants such as ozone (O_3) and nitrogen oxides (NO_X = nitric oxide (NO) + nitrogen dioxide (NO_2)) within forest canopies, substantial chemical reactions can occur in the air volume occupied by forests (Makar et al., 1999; Strong et al., 2004). For example, reactions of biogenic hydrocarbons with O_3 can form substantial amounts of hydroxyl radical (HO) which can in turn augment the rates of biogenic hydrocarbon destruction within and above plant canopies (Makar et al., 1999; Stroud et al., 2005; Sillman et al., 2002; Tan et al., 2001).

While studying photochemical processes within and immediately above forest canopies it is crucial to consider the difference between the chemical species lifetimes and turbulence time scales. For chemical species whose lifetimes are less than or similar to the turbulence time scales, the photochemical processing within and immediately above forest canopies can modify the actual flux density of hydrocarbons entering the overlying atmospheric boundary layer. For tall and dense forests, earlier studies (Gao et al., 1993; Makar et al., 1999; Stroud et al., 2005) indicate that significant photochemical activity can take place within canopies. Such photochemical activity can

be sufficiently strong to modify the biogenic hydrocarbon concentration profiles within and above forests (Holzinger et al., 2005). Therefore, for those hydrocarbons (e.g., terpenes) whose chemical lifetimes are shorter than the atmospheric turbulence time scales, emission rates determined from leaf-based information may not reflect the true material flux entering the atmospheric boundary layer (Forkel et al., 2006). Model estimates demonstrate that chemical reactions within forests can reduce the emission fluxes of biogenically emitted volatile organic compounds from 10 to 40% from the emission fluxes of the tree branches (Makar et al., 1999; Stroud et al., 2005). For short-lived species such as β-caryophyllene, approximately 70% of the locally produced chemical species can be photochemically destroyed within forest canopies (Stroud et al., 2005; Fuentes et al., 2000). Due to more effective surface deposition processes, the fate of reaction products can substantially differ within the canopy compared to the free atmosphere where products can experience further oxidation.

It is well known that biogenically emitted hydrocarbons have strong effects on the regional and urban production of secondary air pollutants (Chameides et al., 1988). Consequently, biogenically emitted hydrocarbons are treated in urban and regional air quality models and ordinarily these emissions are estimated from measurements made at the foliage level. The emissions are treated in air quality models that make their calculations using grids of 4 km by 4 km or larger. Because of neglect of in-canopy chemical processing, this practice may lead to errors in model forecasts of ozone and particle production. Therefore, the principal motivation of the present study is to use a detailed field measurement dataset from a forest to examine the significance of the chemical processing that occurs in the canopy. A high level of chemical processing in the canopy may cause a large difference between the emission rates of biogenic hydrocarbon at the foliage level and the subsequent, actual emissions to the regional scale.

The in-canopy chemical processing effects should be most pronounced in suburban and rural areas under the influence of forested ecosystems capable of high rates of emission of biogenic volatile organic compounds (BVOC). Therefore, in this manuscript we report findings from field and numerical modeling investigations of the degree of chemical processing within a mixed deciduous forest in the southeastern United States, which is known to emit large amounts of BVOC such as isoprene and monoterpenes, with noontime peak flux densities exceeding 50 nmol (isoprene) m^{-2} s^{-1} (Baldocchi et al., 1995). In this manuscript we quantify the degree and rates of BVOC chemical processing for this mixed deciduous forest under the influence of ambient NO_x levels produced from heavy suburban traffic. This was accomplished by combining observations of the diurnal and vertical profiles of BVOC, O_3, and NO_X, with photochemical modeling to estimate intra-canopy dynamics in the production of secondary oxidants such as O_3, HO, nitrate radicals (NO_3), and peroxy radicals (HO_x = HO + hydroperoxy radicals (HO_2)). A key characteristic of the data analysis was to use a chemical box model as a data assimilation tool. The hydrocarbon measurements were 1-h averages that were used to reinitialize the model every hour. The model was used to quantify the relative importance of the sources of HO_x as functions of altitude along with the destruction rates of isoprene and the principal monoterpenes. Finally, the production rates of methacrolein and methyl vinyl ketone were examined. The results of this study demonstrate that in forested areas it may not be valid to use unprocessed biogenic emissions estimated from measurements made at the foliage level for regional scale air quality modeling. Regional-scale air quality models should include chemical preprocessing of biogenic hydrocarbons in order to accurately represent the photochemical production of ozone and other pollutants.

2 Methodology

Air chemistry and micrometeorological measurements were made from 15–22 July 1999 at the United States Department of Energy reservation near Oak Ridge, TN (35°57′30″N, 84°17′15″W; 335 m above sea level, an AmeriFlux site). The forested site is classified as a mixed-species, broad-leaved deciduous forest. The dominant tree species at the site included oak (*Quercus alba* L., *Quercus prinus* L.), hickory (*Carya oata*), maple (*Acer rubrum* L., *Acer saccharum*), tulip poplar (*Liriodendron tulipifera* L.), black gum (*Nyssa sylvatica Marsh*) and loblolly pine (*Pinus taeda* L.). A survey was conducted during 1999 to study tree densities within the flux footprint of the 50-m scaffolding tower that was used to make measurements. The average composition along the established transects, on a basal area basis, was 14% pine, 16% maple, 41% oak and 13% other deciduous species (Wilson et al., 2001). Oaks and tulip poplars were the most important hydrocarbon-emitting tree species, with high amounts of isoprene emissions, although pines were also significant contributors with high monoterpene emissions. The total forest leaf area index for this 26-m forest (h_c) was 6.0 (Baldocchi et al., 1995). The forest atmosphere was influenced by anthropogenic pollutant emissions from automobiles on a road located approximately 1.6 km from the site. During the morning (0630 to 0900 hours) and afternoon hours (1500 to 1700 hours), the traffic of light vehicles impacted the atmosphere at the measurement site as confirmed from unusually elevated concentrations of NO_X.

2.1 Micrometeorological measurements

As part of the ongoing investigations at the Oak Ridge site, water vapor (Wilson et al., 2001), sensible heat flux and state variables were continuously measured. Wind speed and direction were measured at 45 m above the ground, using a propeller anemometer (model 05701, RM Young Co., Rapid City, MI). Net radiation measurements were made at 45 m above the ground using a net pyrradiometer (model S-1, Swissteco Pty., Ltd., Melbourne, Victoria, Australia). Photosynthetically active radiation (PAR) was measured with a quantum sensor (model LI-190S, Li-Cor Inc., Lincoln, NB) within (at 0.2 m) and above (at 25.6 m) the canopy. Air temperature and relative humidity were measured at 36.6 m above ground (model HMP-35A, Vaisala, Finland). This sensor was shielded from the Sun and aspirated to prevent condensation. Ancillary meteorological data were acquired with and stored in data loggers (model CR21X, Campbell Scientific Inc., Logan, UT). The sensors were sampled every second and half-hour averages were computed and stored on a computer, to coincide with the eddy covariance flux measurements. The eddy-covariance method was used to measure flux densities of isoprene (at 39.9 m) employing a three-dimensional sonic anemometer (model SAT-211/3K, Applied Technology Inc., Boulder, CO) and an ozone-induced chemiluminesence instrument (FIS, Hills Scientific, Boulder, CO). Also, from the sonic anemometer data the friction velocity (u^*) was estimated based on the momentum fluxes (τ). The u^* (= $[\tau/\rho]^{0.5}$, ρ is the air density) provided a measure of atmospheric turbulence above the forest canopy. Wilson et al. (2001) provide additional information on the measurements at the Oak Ridge tower site.

The residence times of air parcels, emanating at different depths of the canopy and ending at the flux measurement point (39.9 m above ground), were estimated with the aid of a Lagrangian diffusion model (Baldocchi 1997; Strong et al., 2004). Marked fluid particles (5000) were released from selected canopy depths and allowed the particles to be displaced throughout the landscape according to the nature of the turbulent characteristics

as described by the model. For each fluid particle, the displacement was estimated and then ensemble statistics of air parcel residence times were determined.

2.2 Air chemistry measurements

Ambient levels of 89 hydrocarbon compounds, O_3, and NO_X were measured at six levels (0.2, 9.4, 17.7, 25.6, 31.5 and 39.9 m) above the forest floor. Gas profile measurements were accomplished with a single gas analyzer, made possible through the use of manifold system and sequential canister air samplers from individual intakes. A pumping system was used to continuously draw atmospheric air through cleaned Teflon tubing (12.7 mm ID, 70 m length) from the air intakes at six levels at flow rates >10 L min^{-1} (the air sampling tubing was cleaned in the laboratory by passing distilled water though the tubing, followed by evacuation with a pump while the line had a filter at the inlet). A manifold system allowed sub-sampling of a single level at a time from these lines. The high flow of air was required to reduce the residence time of air in the tubing. Teflon filters (pore size 1 μm) were installed at the inlet of sampling lines to remove pollen and dust, and to keep sampling lines clean. Ozone measurements were made with an ultraviolet light absorption-based instrument (model 49C, Thermo Environmental Instruments Inc., Franklin, MA). Nitric oxide (NO) and nitrogen dioxide (NO_2) measurements were made with a chemiluminescence instrument (model 42C, Thermo Environmental Instruments Inc., Franklin, MA). The O_3 and NO_X measurements were made simultaneously while the profile manifold was sampling a particular level.

For the hydrocarbon compounds, a portion of the sampled air was directed by automatic samplers (910A sampler and 912 sequential adapters, XonTech Inc., Van Nuys, CA) into evacuated canisters. These samples were collected in 3.2 L electropolished, stainless steel canisters (Biosphere Research Corp., Hillsboro, OR) to determine the ambient levels of hydrocarbons. The air samplers were equipped with mass flow controllers that allowed constant airflow rates (100–150 mL min^{-1}) into the canisters. The integrated air samples stored in canisters were analyzed at the study field site within 24 hours after sample collection or returned to the laboratory and analyzed within two weeks after sample gathering.

Because hydrocarbons in ambient air were in trace amounts, the samples required water removal and pre-concentration prior to sample analysis. At the study field site, a 2-m Teflon loop (3.175 mm OD) kept at −10°C was used to remove water from samples and thus reduce water-related peak retention time variations. The dried air samples were cryogenically cooled to concentrate hydrocarbon compounds. The cryogenic trap was packed with 60/80 mesh untreated glass beads, and cooled at −150°C. Air samples of known volume (regulated by a mass flow controller, model Tylan FC-260, Mykrolis Corp., Billerica, MA) were concentrated by passing air through the dryer and subsequent cryogenic trap. Concentrated samples were introduced to the chromatograph column via a six-port valve and by rapidly heating the trap to 150°C. The hydrocarbons were separated using a fused silica capillary column (HP-1, 60 m, 0.32 mm ID, 1.0 um film thickness, Hewlett Packard). The column carrier gas was helium, flowing at 2 ml min^{-1}. The samples were analyzed with a gas chromatograph (GC, Model 6890, Hewlett Packard, Pal Alto, CA) furnished with a mass selective detector (Model 5972 MSD, Hewlett Packard). In the laboratory, an automated pre-concentration system (model EnTech 7000 with 7016 auto-sampler, Entech Instruments Inc., Simi Valley, CA), employing three-stage micro purge and trap techniques for water removal, was interfaced with GC-MSD (GC model 6890 and MSD model 5973, Hewlett Packard). The GC-MSD system operated in selected ion

monitoring (SIM) mode that allowed identification and quantification of target compounds based on retention times and relative abundance of selected ions. Two ions were measured for each of the target compounds. The SIM technique was highly specific and sensitive. Both GC-MSD systems were calibrated using standard mixtures prepared in the laboratory using multi-component liquid and gas mixtures (Scott Specialty Gases, Plumsteadville, PA). Standard mixtures were prepared by a gravimetric method, diluted with ultra-cleaned humidified air and then stored in electropolished polished canisters. Prepared standard concentrations were verified with National Institute of Standards (NIST) 1800 (15 compounds) and NIST 1804 (19 compounds) hydrocarbon standards. The analytical precision of the determination of the hydrocarbon concentrations was 5% as established from multiple measurements made on individually selected air samples (Fuentes and Wang, 1999).

2.3 Photochemical modeling

To investigate the hydrocarbon chemical processing within and above the forest canopy, a box model was applied for the time period (1400–1900 hours) considered to be most photochemically active on a single day (July 20), which was representative of the chemical species measurements we made throughout the eight-day campaign. The Regional Atmospheric Chemistry Mechanism, RACM1, (Stockwell et al., 1997) was revised (RACM2) and our modeling was based on the revised version. The revised RACM2 included a total of 108 chemical species in 293 reactions, of which 29 were photochemical reactions. The new reactions included explicit photochemical schemes for acetone (ACT), methyl ethyl ketone (MEK), methyl vinyl ketone (MVK), higher ketones (KET), and the treatment of three newly aggregated dicarbonyl species formed from the oxidation of aromatic chemical species (diethyl ketone was chosen to represent the higher ketones). The chemistry of aromatic species was based on the scheme reported by Calvert et al. (2002). The isoprene mechanism was adopted from that reported by Geiger et al. (2003), and additional modifications were made to explicitly include the chemistry of methyl vinyl ketone. The chemistry of α-pinene and d-limonene was also included in the modified RACM2 (Stockwell et al., 1997), with the d-limonene plus HO reaction rate taken from Gill and Hites (2002) and the reaction products of α-pinene- and d-limonene-generated peroxy radicals with the NO taken from Atkinson and Arey (2003). The effects of clouds, aerosols and other atmospheric attributes affecting the disposition of actinic flux were incorporated in the model as discussed below.

The RACM2 consists of grouped chemical species that represent the chemistry of classes of organic compounds. A procedure was employed to aggregate the measured hydrocarbon compounds following the same one employed in the original RACM2 (Stockwell et al., 1997). The photochemical mechanism included methane (CH_4), ethane (ETH), and three levels of higher alkanes, HC3, HC5, and HC8, with average carbon numbers of 3, 5 and 8, respectively. Aromatic chemical species were represented by toluene (TOL), benzene (BEN), and more reactive aromatics such as xylene (XYL). In the RACM2, the alkenes included ethene (ETE), alkenes with the double bond at the end of the molecule (OLT), alkenes with the double bond not at the end of the molecule (OLI), butadiene (DIEN), and other anthropogenic dienes. The biogenic volatile organic compounds (BVOC) included isoprene (ISO), α-pinene (API), and d-limonene (LIM). Isoprene reaction products methacrolein (MACR) and methyl vinyl ketone (MVK) were also included in the photochemical mechanism. Field measurements for formaldehyde

(HCHO) and acetaldehyde (ALD) were not available; based on past summer-time field measurements over forested environments (Sumner et al., 2001), we assumed these levels to be 1.0 and 0.5 ppbv, respectively. This was a conservative choice that may underestimate the relative importance of HCHO photolysis as a source of HO_2 in the forest canopy.

The RACM2 and its predecessors the Regional Acid Deposition Mechanism and RACM1 have been tested and validated against measurements (e.g., Stockwell et al., 1997, 1990). Therefore, the purpose of the modeling was to estimate the loss rates of biogenic hydrocarbons as affected by the chemical reactions with O_3, HO, and NO_3. In addition, the production rates of methacrolein and methyl vinyl ketone were determined from the photooxidation of biogenic hydrocarbons. At the beginning of every hour the model was initialized with hourly averaged, measured mixing ratios of O_3, NO, NO_2, H_2O, and hydrocarbons. Specifically, the following RACM2 hydrocarbon chemical species were included in the initialization: HC3, HC5, HC8, OLT, OLI, DIEN, TOL, XYL, ISO, MACR, MVK, API, and LIM. For the chemical species CO, CH4, H_2 (hydrogen), O_2 (oxygen), and N_2 (nitrogen), continental background levels were assumed in the model. The mixing ratios for HCHO and ALD were initialized in the model as discussed. By reinitializing the model with measured chemical species at hourly intervals, the measurements provided a series of realistic simulations cases that were used to calculate the chemical processing within the forest canopy.

The photolysis rate parameter of the ith chemical species χ (J_χ) is the integral of the spectral actinic flux, $I(\lambda)$, spectral cross-section as a function of temperature $\sigma_\phi(\lambda, T)$, and spectral quantum yield as a function of temperature, ϕ_χ (λ, T), for the wavelengths (λ) of interest (from λ_1 to λ_2):

$$J_\chi = \int_{\lambda_1}^{\lambda_2} \sigma_\chi(\lambda, T)\phi_\chi(\lambda, T)\mathrm{I}(\lambda)\partial\lambda \tag{1}$$

Measurements of $I(\lambda)$ were not available but PAR was measured at the top and floor of the forest canopy. Therefore, the measurements of PAR were used to scale model-calculated photolysis rate coefficients. The first step was to use a radiative transfer model (Madronich, 1987) to estimate the 23 RACM2 photolysis rate coefficients (J_i) for cloudless conditions for every hour simulated. The radiative transfer model computed $I(\lambda)$ using the delta-Eddington approximation (Joseph, 1976) and both $\sigma_\chi(\lambda, T)$ and ϕ_χ (λ, T) were determined based on published results (Stockwell et al., 1997). RACM2 includes several new photolyzed species including acetone, methyl ethyl ketone, methyl vinyl ketone and an aggregated dicarbonyl species produced by aromatic oxidation. For RACM2 the revised photolysis rate parameters J_{acetone}, $J_{\mathrm{methyl\_ethyl\_ketone}}$, and J_{ketone} differed from the RACM1 J_{ketone} by factors of 0.1949, 1.304 and 0.8246, respectively. The $J_{\mathrm{dicarbonyl}}$ was taken to be equal to $J_{\mathrm{methylglyoxal}}$ and $J_{\mathrm{methyl\_vinyl\_ketone}}$ was insignificant within the lower depths of the forest canopy. For every hour all of the calculated photolysis rate coefficients, J_i, and the photolysis rate coefficient of acetaldehyde, J_{ALD}, were represented by ratio (J_i/J_{ALD}) and used for further calculations in step 6 (see below). It was important to calculate J_i/J_{ALD} for each hourly time interval because this ratio was time dependent for some chemical species.

The effects of clouds, aerosol scattering, O_3 absorption and shading within the forest canopy complicated the estimation of the photolysis rate coefficients. The second step used the 30-min averaged measurements of PAR made near the forest floor at 0.2 m and at the top of the canopy at 25.6 m to estimate the altitude-dependent PAR_z above and within the

canopy. Beer's law was applied and the measured PAR measurements were used to estimate the total light absorbance (A_{Tot}) of the PAR in the forest canopy:

$$A_{\mathrm{Tot}} = \ln\left(\frac{PAR_{0.2\mathrm{m}}}{PAR_{25.6\mathrm{m}}}\right) \tag{2}$$

Equation 3 was used to estimate the total light absorbance, A_z, at any altitude within the canopy. The variable $f_{\mathrm{path\_length}}$ represented the fractional path that the light traveled through the forest canopy; $f_{\mathrm{path\text{-}length}}$ was 0% at the canopy top and 100% at the forest floor.

$$A_z = A_{\mathrm{Tot}} \times f_{\mathrm{path\_length}} \tag{3}$$

The altitude-dependent PAR_z was estimated from the measured PAR at the top of the canopy, the total altitude-dependent absorbance, and the solar zenith angle (ϕ):

$$PAR_z = \frac{PAR_{25.6m}}{\cos(\phi)} \exp(A_z) \tag{4}$$

The photochemical simulations were made for layers at the following heights: 39.8, 31.5, 25.6, 17.7, 9.4, and 0.2 m. The first three heights were at or above the forest canopy so it was assumed that PAR_z was equal to $\mathrm{PAR}_{25.6\ \mathrm{m}}$. For heights within the canopy (17.7, 9.4 and 0.2 m) $f_{\mathrm{path\text{-}length}}$ was 31.1, 63.8 and 100%, respectively.

Step 3 established a relationship between PAR and the photolysis rate parameter of acetaldehyde. The actinic flux for the "best estimate surface albedo" (Finlayson-Pitts and Pitts, 1998) and equation 1 were used to estimate the photolysis rate parameter for acetaldehyde for a solar zenith angle of 0° ($J_{\mathrm{ALD}-0^\circ}$). PAR for these same conditions, PAR_{0°, was approximated by integrating the actinic flux between 400 and 680 nm. The ratio $J_{\mathrm{ALD}-0^\circ}/\mathrm{PAR}_{0^\circ}$ was calculated and used in step 4. In step 5, the altitude- dependent PAR_z and the ratio $J_{\mathrm{ALD}-0^\circ}/\mathrm{PAR}_{0^\circ}$ were required to calculate the photolysis rate coefficient of acetaldehyde at the times and altitudes within and above the canopy to be modeled:

$$J_{\mathrm{ALD-PAR}} = \frac{J_{\mathrm{ALD}-0^\circ}}{PAR_{0^\circ}} PAR_z \tag{5}$$

Finally in step 6, all the photolysis rate coefficients for RACM2 that were calculated from the radiation model for clear sky conditions were adjusted according to the measured PAR. The RACM2 coefficients were calculated from the product of J_i/J_{ALD} calculated in step 1 and $J_{\mathrm{ALD\text{-}PAR}}$:

$$J_{i-\mathrm{PAR}} = \frac{J_i}{J_{\mathrm{ALD}}} J_{\mathrm{ALD-PAR}} \tag{6}$$

3 Results and Discussion

The measurements reported in this study were obtained under partly cloudy conditions. The PAR measured above the forest canopy only reached maximum values of about 1,000 μmol $\mathrm{m}^{-2}\ \mathrm{s}^{-1}$ whereas at the forest floor the peak PAR levels only reached 100 μmol $\mathrm{m}^{-2}\ \mathrm{s}^{-1}$. Air temperature measured at 36.6 m above the forest experienced maximum values of 28°C during the 1500 to 1700 hours (Figure 1). The most intense atmospheric turbulence was

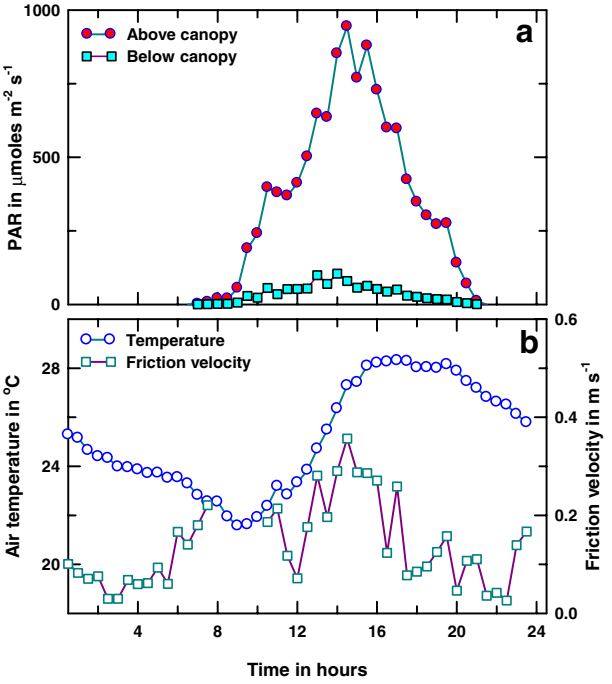

Figure 1 Diurnal variations of (**a**) photosynthetically active radiation (PAR) above (•) and below (♦) the forest canopy (*top panel*), and (**b**) air temperature (o) measured at 36.6 m above a mixed deciduous forest canopy, and friction velocity (□) determined at 39.9 m above the ground at Oak Ridge, TN on 20 July 1999.

observed during 1300 to 1700 hours when the friction velocity reached maximum values of approximately 0.4 m s^{-1}. As discussed below, these atmospheric conditions promoted substantial photochemical activity as revealed by the amounts of secondary oxidants estimated from the reactions involving biogenic hydrocarbons.

The investigated forest was deep (26-m tall) and had a large leaf area index (6.0), with most of the foliage confined between 18 and 26 m above the ground. These attributes permitted relatively long residence times for the air parcels emanating from the lower depths of the forest. For example, on average air parcels emanating from 3–10 m above the ground remained within the forest 8 min, with maximum residence times reaching 30–40 min. As expected, air parcel traveling from the forest crown had shorter residence times, reaching maximum values of 1–10 min (Figure 2). To establish a conservative lower limit of air residence times, the simulations were made with the Lagrangian model treating high levels of atmospheric turbulence (u^*=0.65 m s^{-1}). Therefore, the Lagrangian modeling established that air parcel residence times within the forest canopy were sufficiently long for chemical reactions to occur.

For the day included in the modeling studies (20 July 1999), oxidant levels were considered 'moderate' as revealed by ambient O_3 levels which exhibited maximum mixing ratios of 80 ppbv (Figure 3). Above the forest canopy (at 39.8 m above ground) O_3 mixing ratios were consistently higher than those within the forest canopy (at 0.2 above the surface), where maximum O_3 mixing ratios attained 40 ppbv. The peak O_3 levels at both heights coincided with the period of maximum late-day photochemical activity, presumably driven by the local horizontal transport of NO_X which had occurred earlier in the day. During the period of 1400 to 1900 hours, the difference between O_3 levels above and within the forest canopy exceeded 30 ppbv. This substantial O_3 drawdown occurred while the forest canopy remained strongly coupled to the overlying atmosphere as evidence by

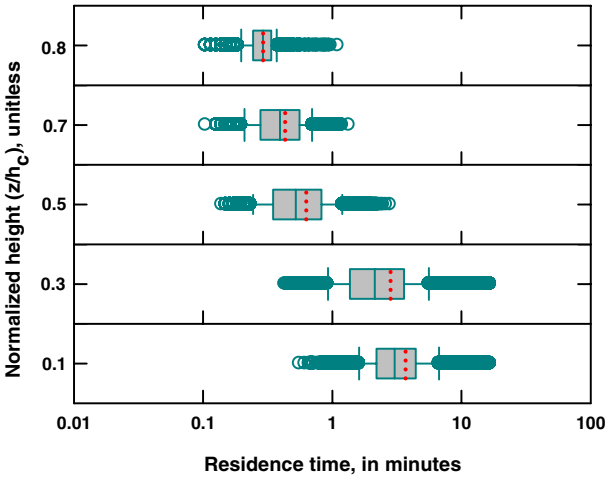

Figure 2 Air parcel residence times estimated for selected heights (z/hc = 0.1, 0.3, 0.5, 0.7, and 0.8; hc is the canopy height of 26 m) using a friction velocity (*above the canopy*) of 0.65 m per second. For the box plots, the *dotted line* is the mean, the *thin line* is the median, the *shaded box* shows the inner-quartile range, the *error bars* denote the 10th and 90th percentiles, and outlier data are shown as *circles*.

strong atmospheric turbulence, which routinely remained high throughout the afternoon (Figure 1). The large O_3 removal was the result of dry deposition to the forest (Fuentes et al., 1992; Sigler et al., 2002) and photochemical processes occurring within the volume occupied by the forest canopy.

Ambient levels of NO_X exhibited strong diurnal patterns, with maximum mixing ratios reaching 8 ppbv in the early morning hours, followed by a second smaller peak in the late afternoon (Figure 4). The local traffic, on a road located approximately 1.6 km south from the study site, may have impacted the NO_x measurements. Ordinarily the ambient NO_X levels above the forest canopy were greater than those measured within the canopy (Figure 4). However, following periods of high local traffic (as revealed from personal observations during 0600 to 0800 and 1500 to 1700 hours), NO_x levels inside the forest exceeded values above the canopy. The higher NO_X levels within the canopy than above the forest may have resulted from the contribution of both NO soil emissions and transport of NO_X. Generally, the NO_x levels above and within the canopy track each other well. During the afternoon photochemical simulation period, the NO_x levels used to initialize hourly model runs ranged from 1 to 4 ppbv.

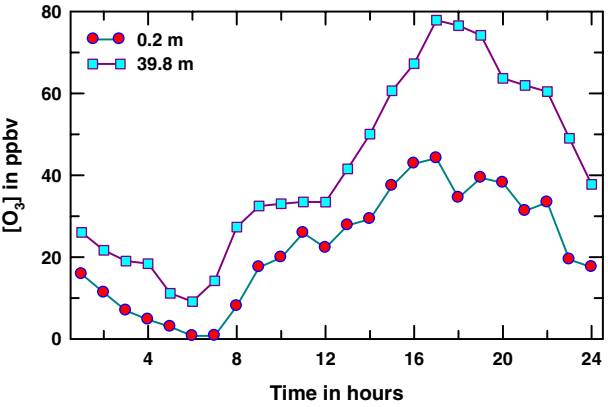

Figure 3 Diurnal variations of ozone mixing ratios measured within and above a mixed deciduous forest canopy at Oak Ridge, TN on 20 July 1999.

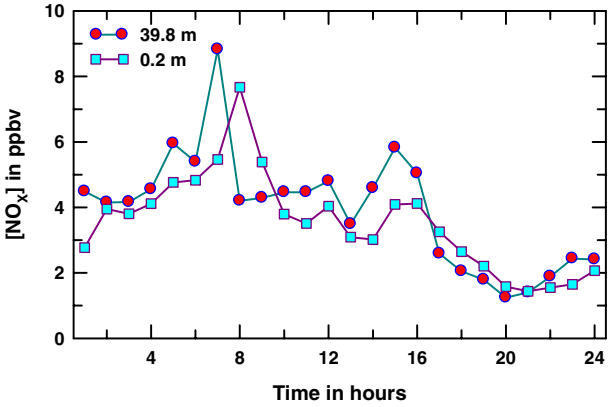

Figure 4 Diurnal variations of nitrogen oxide mixing ratios measured within and above a mixed deciduous forest canopy at Oak Ridge, TN on 20 July 1999.

Isoprene flux densities measured above the forest exhibited strong diurnal patterns, with isoprene flux densities near zero in the early morning and evening hours and peak fluxes of nearly 60 nmol (isoprene) m^{-2} s^{-1} in the early afternoon (Figure 5). Occasional periods of isoprene deposition to the canopy or short-term suppression of isoprene flux densities were detected. For the Walker Branch forest, Baldocchi et al. (1995) also reported reduced isoprene flux densities during the early afternoon. Based on isoprene concentration gradients (data not shown), reduced flux densities occurred when isoprene-rich air masses were transported to the study site from neighboring tracts with higher densities of oak trees. This was supported by our observations that isoprene mixing ratios at the top of the tower were greater than the quantities measured close to the forest canopy. The patterns of isoprene fluxes (Figure 5) were consistent with those reported for forests in which the isoprene source is heterogeneously distributed throughout the landscape (Fuentes et al., 1996; Baldocchi et al., 1995; 1999). For heterogeneous forests, isoprene fluxes not only vary with time of day but also change with wind direction because of the spatial variability in the source strength (Kaharabata et al., 1999). For the studied forest not all trees were isoprene emitters, and hence spatial variation of emitters and non-emitters within the tower footprint influenced the temporal patterns of observed isoprene levels. During the study period, the source strength of isoprene production from the forest surrounding the tower was sufficiently strong to yield maximum ambient isoprene mixing ratios exceeding 12 ppbv (Figure 6).

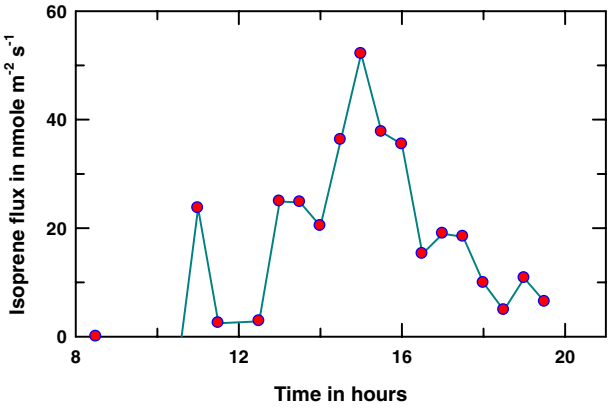

Figure 5 Diurnal variation of isoprene flux density measured above a mixed deciduous forest canopy at Oak Ridge, TN on 20 July 1999.

For the selected modeling period, maximum ambient isoprene levels of 12 ppbv were measured within the forest crown (Figure 6). Isoprene levels decreased with height away from the main canopy source in response to turbulent transport and chemistry. In contrast, O_3 levels monotonically decreased with canopy depth. During the modeling period, NO_X remained almost invariant with canopy depth and levels ranged from 2 to 6 ppbv. The observed O_3 and NO_X levels were indicative of a moderately polluted air mass whose chemical attributes had contributions from suburban and rural forested atmospheres. This is comparable with other rural sites that are affected by suburban atmospheres such as the PROPHET (Program for Research on Oxidants: Photochemistry, Emissions and Transport) field site located in rural Michigan. In past studies, the PROPHET site had ambient O_3 levels ranging from 20 to 80 ppbv and NO_x levels between 250 pptv and 2.5 ppbv (Thornberry et al., 2001). Urban regions generally experience NO_x levels that are substantially greater than those found over forested environments. For example, the mean NO_x mixing ratios in Los Angeles range from 50 to 100 ppbv while the mean maximum O_3 mixing ratios range from 40 to 120 ppbv (Fujita et al., 2003).

In terms of carbon mass, the measured BVOCs and the isoprene photooxidation products, methacrolein and methyl vinyl ketone (Figure 7), comprised over 75% of the measured hydrocarbon loading. The methacrolein and methyl vinyl ketone levels reached their maximum values within the vicinity of forest crown. As discussed below, the patterns of methacrolein and methyl vinyl ketone variations with altitude suggest that the availability of these compounds was strongly influenced by the local chemistry. The averaged values for methacrolein and methyl vinyl ketone above the forest canopy were similar in magnitude to previously published results for forested environments (Montzka et al., 1993, 1995). Figure 8 shows the mixing ratios of the VOCs as aggregated into chemical species considered in the photochemical model. At all heights, the mixing ratio of isoprene was nearly an order of magnitude higher than the other VOCs. The second and third most abundant chemical species included isoprene oxidation products methacrolein and methyl vinyl ketone. The mixing ratios of α-pinene and d-limonene were between two and three orders of magnitude lower than for isoprene. The composition of anthropogenic VOCs was representative of aged urban emissions with the mixing ratios of alkanes greater than the mixing ratios of the anthropogenic alkenes. Although the measured ambient levels of VOCs varied in time, overall the total mixing ratio of the measured hydrocarbons reached near 80 ppbC near the forest floor (Figure 8). The VOC mixing ratio reached about 90 ppbC within the forest crown and declined to approximately 50 ppbC above the forest canopy. This gradient was driven primarily by variations in isoprene (Figure 6) and its oxidation products (Figure 7). High VOC to NOx (VOC/NOx) ratios were associated with rapid rates

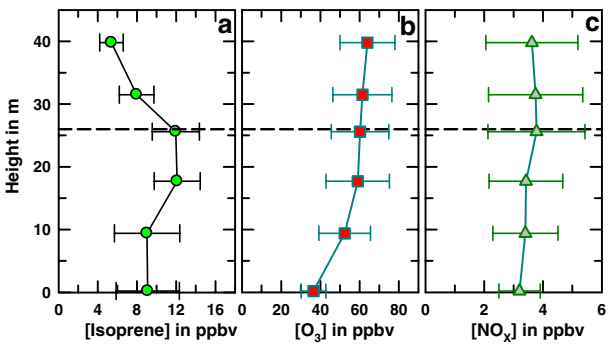

Figure 6 Averaged vertical variations of (**a**) ozone, (**b**) nitrogen oxide, and (**c**) isoprene mixing ratios within and above a mixed deciduous forest canopy at Oak Ridge, TN on 20 July 1999 during 1400 to 1900 hours (local time). The *error bars* denote one standard deviation from the mean mixing ratios.

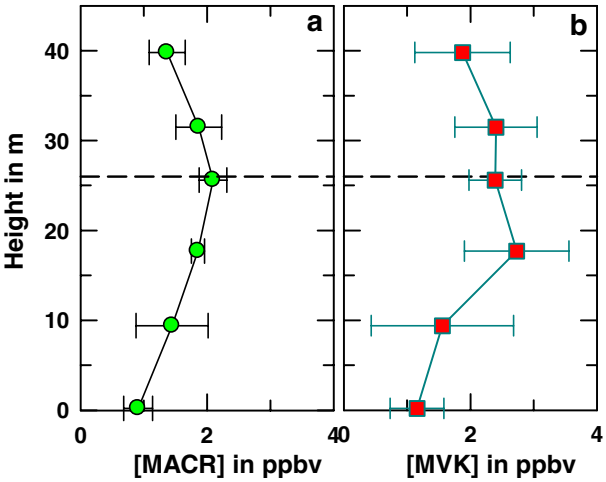

Figure 7 Averaged vertical variations of (**a**) methacrolein (MARC) and (**b**) methyl vinyl ketone (MVK) mixing ratios within and above a mixed deciduous forest canopy at Oak Ridge, TN on 20 July 1999 during 1400 to 1900 hours (local time). The *error bars* denote one standard deviation from the mean mixing ratios.

of O_3 formation as determined from the model. At the study site, the VOC/NOx ratio was relatively high compared to urban environments, with values exceeding 20 ppbC/ppbN within the forest canopy. The ratios reached peak levels at the top of the canopy and then declined to near 10 ppbC/ppbN above the canopy.

The central goal of this study was to quantify the rates of chemical processing of BVOCs within and above the forest canopy during the daytime period when NO_x emissions from nearby suburban roadways were high. The three most important photochemical reactions leading to isoprene destruction involve reactions with O_3, HO, and NO_3. One path for the production of HO radicals is O_3 photolysis (R1) and the subsequent reaction of excited atomic oxygen, $O(^1D)$, with water vapor (H_2O) (R3). Note that only a small percentage of the $O(^1D)$ react with H_2O due to its quenching to the ground state, $O(^3P)$, by nitrogen and/or oxygen molecules (M) and the subsequent reaction of $O(^3P)$ to reform O_3 (reactions R1-R4).

$$O_3 + h\nu \rightarrow O(^1D) + O_2 \quad (R1)$$

$$O(^1D) + M \rightarrow O(^3P) + M \quad (R2)$$

$$O(^3D) + O_2 + M \rightarrow O_3 + M \quad (R3)$$

$$O(^1D) + H_2O \rightarrow HO + HO \quad (R4)$$

The photolysis of formaldehyde (HCHO) in the presence of NO is another important source of HO radicals. Formaldehyde has two photolysis reactions: one produces the molecular products of hydrogen (H_2) and carbon monoxide (CO), while the other produces formyl radicals (HCO) and a hydrogen atom (H) that can lead to the production of HO_2 radicals (reaction R5-R8). The HO_2 radicals can undergo reactions with NO to form NO_2 (R9). Additionally, the HO_2 radicals can react with O_3 to form HO and molecular oxygen (R10)

$$HCHO + h\nu \rightarrow H_2 + CO \quad (R5)$$

$$HCHO + h\nu \rightarrow HCO + H \quad (R6)$$

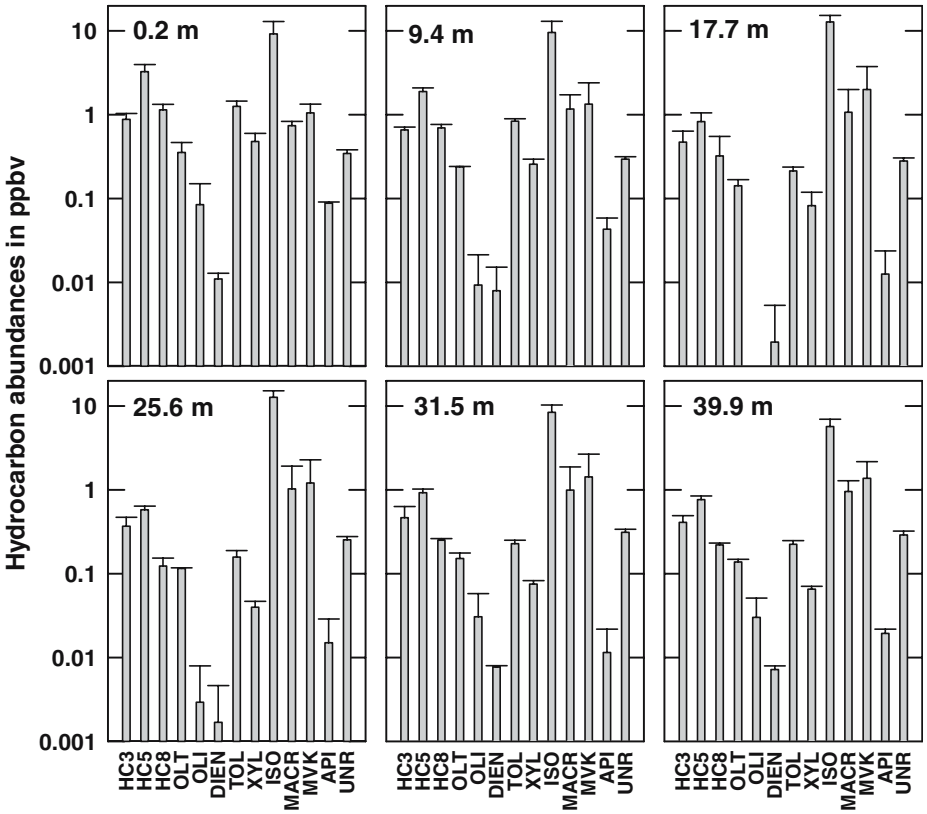

Figure 8 Mixing ratios of speciated hydrocarbon compounds measured within and above a mixed deciduous forest canopy at Oak Ridge, TN on 20 July 1999. The level above the ground where measurements were made is indicated by the label inserted for each figure. See text for a description of the compound classes.

$$HCO + O_2 \rightarrow HO_2 + CO \quad (R7)$$

$$H + O_2 \rightarrow HO_2 \quad (R8)$$

$$HO_2 + NO \rightarrow HO + NO_2 \quad (R9)$$

$$HO_2 + O_3 \rightarrow HO + 2O_2 \quad (R10)$$

The photolysis of nitric acid (HNO_3) and nitrous acid (HONO) can yield HO radicals ($HNO_3 + h\nu \rightarrow HO + NO_2$, $HONO + h\nu \rightarrow HO + NO$). Under the conditions considered in this investigation, the HO radical formation from HNO_3 and HONO became negligibly small compared to the other photochemical processes.

The reaction of alkenes with O_3 is another significant source of HO and HO_2 radicals (Finlayson-Pitts and Pitts, 2000). The mechanism of the reaction of O_3 with isoprene (ISO), α-pinene (API) and d-limonene (LIM) consists of several steps that are highly condensed in RACM2.

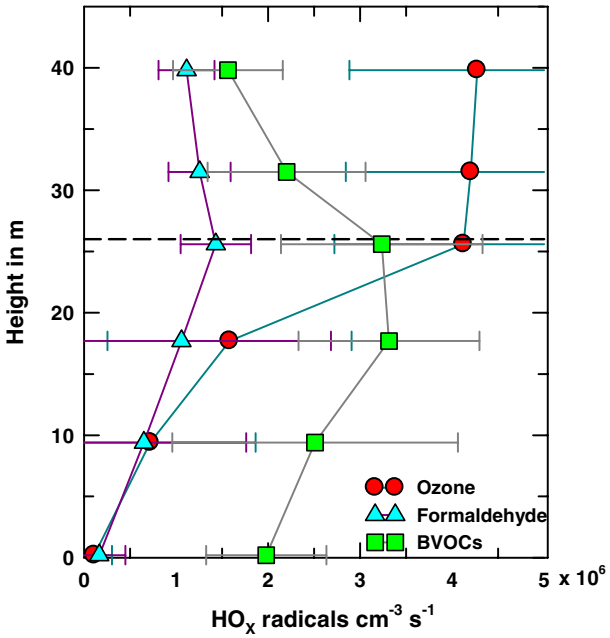

Figure 9 Averaged HO_X radical production rate modeled within and above a mixed deciduous forest canopy at Oak Ridge, TN on 20 July 1999 during 1400 to 1900 hours (local time). The *error bars* denote one standard deviation from the mean mixing ratios. The *dashed line* on the *y*-axis denotes the canopy height.

$$\mathrm{ISO} + \mathrm{O_3} \rightarrow 0.25\,\mathrm{HO} + 0.25\mathrm{HO_2} + \mathrm{Products} \quad \text{(R11)}$$

$$\mathrm{API} + \mathrm{O_3} \rightarrow 0.85\mathrm{HO} + 0.1\mathrm{HO_2} + \mathrm{Products} \quad \text{(R12)}$$

$$\mathrm{LIM} + \mathrm{O_3} \rightarrow 0.85\mathrm{HO} + 0.1\mathrm{HO_2} + \mathrm{Products} \quad \text{(R13)}$$

Above the forest canopy (31.5–39.8 m), O_3 photolysis was the primary source of HO_x radicals (57%), with the reaction of O_3 with BVOC second (25%) and the photolysis of HCHO third (16%) (Figure 9). From the forest crown down to the forest floor the actinic flux rapidly declined, thus decreasing the photolysis rates of O_3 and HCHO. Within the top of the canopy, as the actinic flux was reduced, the reaction of O_3 with BVOC became the greatest source (44%) of HO_x, O_3 photolysis became second (38%) and the photolysis of HCHO remained third (17%). Even lower within the canopy (9.4–0.2 m), the reaction of O_3 with BVOC produced 69% of the HO_x radicals, with O_3 photolysis (13%) and HCHO photolysis (12%) almost equal in importance. However, overall the HO_x production rate decreased from the air above the forest canopy to the forest floor and this caused the HO mixing ratio to decrease within the canopy. HO abundances were close to 0.05 pptv above the forest canopy and decreased to nearly zero at the surface (Figure 10).

The reaction of O_3 with NO_2 is the source NO_3 radicals, R14, and dinitrogen pentoxide (N_2O_5) serves as a reservoir as shown in reaction R15.

$$\mathrm{O_3} + \mathrm{NO_2} \rightarrow \mathrm{NO_3} + \mathrm{O_2} \quad \text{(R14)}$$

$$\mathrm{NO_3} + \mathrm{NO_2} \leftrightarrow \mathrm{N_2O_5} \quad \text{(R15)}$$

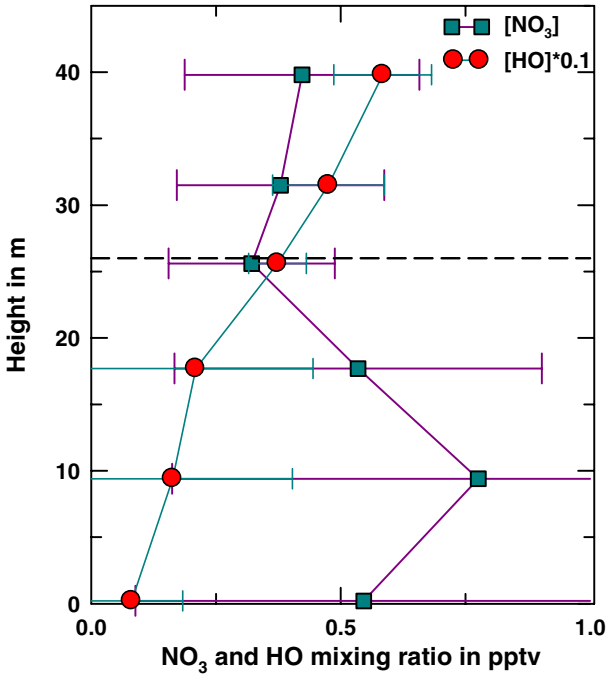

Figure 10 Averaged vertical variations of nitrate and hydroxyl radicals modeled within and above a mixed deciduous forest canopy at Oak Ridge, TN on 20 July 1999 during 1400 to 1900 hours (local time). The *error bars* denote one standard deviation from the mean mixing ratios. The *dashed line* on the *y*-axis denotes the canopy height.

During the daytime the NO_3 can undergo photolysis and is relatively short lived. Within the forest canopy, however, the estimated mixing ratios were substantially higher than the levels determined above the forest canopy (Figure 10). Estimated maximum NO_3 levels reached 1 pptv within the canopy whereas above the forest canopy minimum levels became 0.1 pptv.

Reaction with HO was the dominant destruction mechanism for isoprene. The isoprene reaction rate with HO reached a maximum level near the top of the canopy where the mixing ratios of HO radical and the isoprene were abundant (Figure 11a). The HO levels dropped rapidly within the forest canopy due to lower O_3 photolysis rates and this caused the decrease in the HO-isoprene reaction rate. The reaction rates of isoprene with NO_3 and O_3 were significant but lower than those with HO. The reaction rates of isoprene with NO_3 and O_3 were much more constant with height than the HO reaction rate but these former reaction rates attained maximum values within the forest crown where isoprene mixing ratios were greatest. The patterns of α-pinene and d-limonene destruction rates were much different than those for isoprene (Figures 11b and c). The estimated destruction patterns resulted in part because the rate parameters for the reactions of NO_3 and O_3 with α-pinene and d-limonene were much greater than those for isoprene. The terpene losses were especially high (3×10^5 molecules per second) in the lower canopy where mixing ratios exhibited the highest levels. On average, above the forest canopy, 30 to 40% of the terpenes reacted with HO while the balance reacted with NO_3 and O_3. At the lower levels within the canopy, because of the low concentrations of OH, approximately 60% of the terpenes reacted with NO_3 and 40% reacted with O_3.

The HO radical adds to isoprene and the resulting peroxy radical reacts with NO to produce methacrolein and methyl vinyl ketone (Atkinson and Arey, 2003). The peroxy radical can also react with HO_2 to produce hydroperoxides which subsequently react with

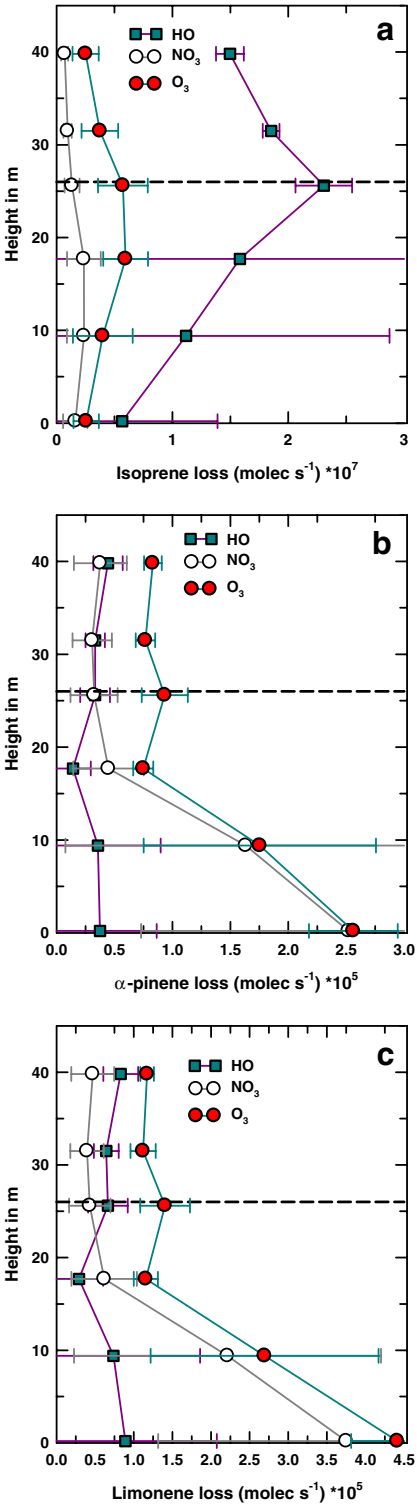

Figure 11 Averaged vertical variations of (**a**) isoprene, (**b**) α-pinene, and (**c**) d-limonene loss modeled within and above a mixed deciduous forest canopy at Oak Ridge, TN on 20 July 1999 during 1400 to 1900 hours (local time). The *error bars* denote one standard deviation from the mean mixing ratios. The *dashed line* on the *y*-axis denotes the canopy height.

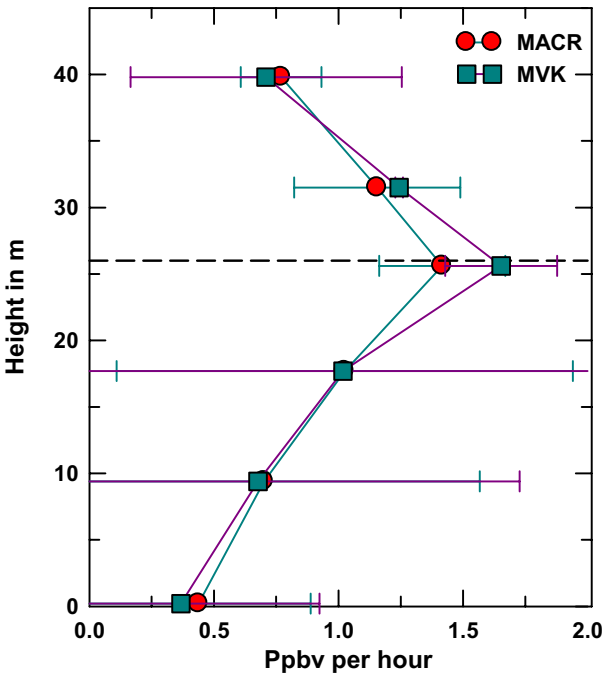

Figure 12 Averaged methacrolein and methyl vinyl ketone production rate modeled within and above a mixed deciduous forest canopy at Oak Ridge, TN on 20 July 1999 during 1400 to 1900 hours (local time). The *error bars* denote one standard deviation from the mean mixing ratios. The *dashed line* on the *y*-axis denotes the canopy height.

HO to form methacrolein and even generate more HO. Methacrolein and methyl vinyl ketone are also produced when O_3 reacts with isoprene. The reaction of NO_3 with isoprene produces several alkyl nitrate compounds (Atkinson, 2000). Similar compounds are produced by the photooxidation of terpenes. For the model results, the greatest rates of methacrolein and methyl vinyl ketone formation occurred within the forest crown in response to the highest ambient levels of both measured isoprene, O_3, and estimated HO radicals (Figure 12). Rates of formation for these oxidative products ranged from 0.5 ppbv per hour in the lower layers of the canopy to 2.0 ppbv per hour within the forest crown. The modeled patterns of methacrolein and methyl vinyl ketone closely resembled the observed levels within and above the forest (Figure 7). These results indicate that the photooxidation of biogenic hydrocarbons represented an important source of methacrolein and methyl vinyl ketone within the forest canopy. The close resemblance of the vertical profiles of ambient levels and production rates of methacrolein and methyl vinyl keton indicatives that within-canopy photochemical processes contributed to the formation of these compounds.

4 Summary and Conclusions

A box model was used to estimate the mixing ratios of HO and NO_3 radicals and to estimate the oxidation rates of isoprene and its production of methacrolein and methyl vinyl ketone from measurements of O_3, NO, NO_2, H_2O and VOC concentrations. The observed VOC to NO_x ratios were relatively high in the forest canopy, higher than those levels ordinarily found in urban environments. Within and above the forest, isoprene and its photooxidation products comprised over 75% of the measured carbon mass and its molar mixing ratio was nearly an order of magnitude higher than the other VOCs. The measured

mixing ratios of methacrolein and methyl vinyl ketone tracked both isoprene levels and HO reaction rates very well with height. The reaction with HO was the dominate loss mechanism for isoprene and its rates of reaction with NO_3 and O_3 were lower but still significant. The reaction rate of HO reached maximum levels near the top of the canopy where the levels of HO radicals and the isoprene were both high. Thus, the vertical profile of HO within the canopy represents a principal determinant of BVOC oxidation, and is in turn determined by changes in the vertical profile of the actinic flux and concomitant changes in the O_3 photolysis rate. The reaction rates of isoprene with NO_3 and O_3 were much more constant with height, compared to the HO reaction rate. The patterns of α-pinene and d-limonene destruction rates were much different than isoprene. Above the canopy, approximately 30 to 40% of these terpene molecules reacted with HO while the balance reacted with NO_3 and O_3; within the canopy approximately 60% of the terpenes reacted with NO_3 and 40% reacted with O_3. Ozone photolysis was the major source of HO_x radicals above the canopy. The production of HO from O_3 and the production of HO_2 from formaldehyde photolysis both declined rapidly within the canopy due to decreasing photolysis rates. The reaction of BVOC with O_3 was the major source of HO within the forest canopy and its rate of radical production reached a peak at the top of the canopy where the ambient O_3 and isoprene levels were both high.

The following conclusions are drawn from this study. First, substantial formation rates of HO and NO_3 radicals can take place in forested environments with moderate to high levels of BVOC production. These radical levels are sufficiently high to drive photochemical reactions within forested environments. Second, substantial methacrolein and methyl vinyl ketone production can take place within the forest canopy. The production rates ranged from 1 to 2 ppbv per hour. Third, for the investigated forest ecosystem the local production of peroxy radicals was relatively high, resulting in intra-canopy levels of 0.6 ppbv. In environments with adequate supply of NO_X, the estimated radical production can control rates of formation of other chemical species such as nitric acid and nitrous acid. The main conclusion from this investigation is that forested ecosystems capable of high rates (>50 nmol m^{-2} s^{-1}) of BVOC emissions, and in the vicinity of modest rates of NOx emissions from suburban automobile traffic, can support a unique and active photochemistry within forest canopies. This chemical processing within forest canopies reduces the mass and chemical reactivity of the BVOCs reaching the regional scale. Neglect of in-canopy processes could lead to an over estimate of ozone production by regional air quality models. Therefore, for forested areas, regional air quality models will likely need to include preprocessing of BVOC emissions to accurately represent the photochemical production of pollutants.

Acknowledgments Fuentes received support from the University of Virginia to carry out the field research of this study. Fuentes also received support from the U.S. National Science foundation (grant ATM-0445012). James Kathilankal of the University of Virginia provided assistance to perform the air parcel trajectory analyses. Tony Delany of the National Center for Atmospheric Research (NCAR) is acknowledged for his able assistance with the NO_X measurements. Kell Wilson from the Atmospheric and Turbulence Diffusion Laboratory, National Oceanic and Atmospheric Administration is thanked for sharing the meteorological data included in this manuscript. Monson and Bowling were supported by a grant from the National Science Foundation and funds from the University of Colorado and the NCAR. Potosnak received support from a National Science Foundation Graduate Research Fellowship. Steve Hoskins provided assisted with the field studies. Stockwell was supported by the NOAA Educational Partnership Program with Minority Serving Institutions (EPP/MSI) under cooperative agreements NA17AE1625 and NA17AE1623. Stockwell and Goliff were supported by the National Aeronautics and 362 Space Administration under the Experimental Program to Stimulate Competitive 363 Research (EPSCoR), grant number NCC5-583. Two anonymous journal reviewers are acknowledged for providing excellent comments to improve the manuscript.

References

Atkinson, R.: Atmospheric chemistry of VOCs and NOx. Atmos. Environ. **34**, 2063–2101 (2000)

Atkinson, R., Arey, J.: Gas-phase tropospheric chemistry of biogenic volatile organic compounds: a review. Atmos. Environ. **37**, 197–219 (2003)

Baldocchi, D.: Flux footprints within and over forest canopies. Boundary-Layer Meteor. **85**, 273–292 (1997)

Baldocchi, D., Guenther, A., Harley, P., Klinger, L., Zimmerman, P., Lamb, B., Westberg, H.: The fluxes and air chemistry of isoprene above a deciduous hardwood forest. Philos. Trans. R. Soc. Lond., A **350**, 279–296 (1995)

Baldocchi, D.D., Fuentes, J.D., Bowling, D.R., Turnipseed, A.A., Monson, R.K.: Scaling isoprene fluxes from leaves to canopies: test cases over a boreal aspen and a mixed species temperate forest. J. Appl. Meteorol. **38**, 885–898 (1999)

Calvert, J.G., Atkinson, R., Becker, K.H., Kamens, R.M., Seinfeld, J.H., Wallington, T.J., Yarwood, G.: The Mechanisms of Atmospheric Oxidation of Aromatic Hydrocarbons. Oxford University Press (2002)

Chameides, W.L., Lindsay, R.W., Richardson, J., Kiang, C.C. :The role of biogenic hydrocarbons in urban photochemical smog – Atlanta as a case-study. Science **241**, 1473–1475 (1988)

Finlayson-Pitts, B.J., Pitts, J.N.: Chemistry of the Upper and Lower Atmosphere. Academic, San Diego, CA (2000)

Fitzjarrald, D.R., Acevedo, O.C., Moore, K.E.: Climatic consequences of leaf presence in the eastern United States. J. Climate **14**, 598–614 (2001)

Forkel, R., Klemm, O., Graus, M. Rappenglûck, B., Stockwell, W.R., Grabmer, W., Held, A., Hansel, A., Steinbrecher, R.: Trace gas exchange and gas phase chemistry in a Norway spruce forest: a study with a coupled 1-dimensional canopy atmospheric chemistry emission model. Atmos. Environ. **40**, 28–42 (2006)

Foster, D.R.: Land-use history (1730–1990) and vegetation dynamics in central New England, USA. J. Ecol. **80**, 753–772 (1992)

Fuentes, J.D., Wang, D.: On the seasonality of isoprene emissions from a mixed temperate forest. Ecol. Appl. 9: 1118–1131 (1999)

Fuentes, J.D., Gillespie, T.J., Den Hartog, G., Neumann, H.H.: Ozone deposition onto a deciduous forest during dry and wet conditions. Agric. For. Meteorol. **62**, 1–18 (1992)

Fuentes, J.D., Wang, W., Neumann,H.H., Gillespie, T.J., Den Hartog, G., Dann, T.F.: Ambient biogenic hydrocarbons and isoprene emissions from a mixed deciduous forest. J. Atmos. Chem. **25**, 67–95 (1996)

Fuentes, J.D., Lerdau, M., Atkinson, R., Baldocchi, D., Bottenheim, J.W., Ciccioli, P., Lamb, B., Geron, C., Gu, L., Guenther, A., Sharkey, T.D., Stockwell, W.: Biogenic hydrocarbons in the atmospheric boundary layer: a review. Bull. Am. Meteorol. Soci. **81**, 1537–1575 (2000)

Fujita, E.M., Stockwell, W.R., Campbell, D.E., Keislar, R.E., Lawson, D.R.: Evolution of the magnitude and spatial extent of the weekend ozone effect in California's South Coast air Basin from 1981 to 2000. J. Air Waste Manage. Assoc. **53**, 802–815 (2003)

Gao, W., Wesely, M.L., Doskey, P.V.: Numerical modeling of the turbulent-diffusion and chemistry of NO_X, O_3, isoprene, and other reactive trace gases in and above a forest canopy. J. Geophys. Res.-Atmos. **98** (d10), 18339–18353 (1993)

Geiger, H., Barnes, I., Bejan, J., Benter, T., Spittler, M.: The tropospheric degradation of isoprene: an updated module for the regional atmospheric chemistry mechanism. Atmos. Environ. **37**, 1503–1519 (2003)

Geron, C., Rasmussen, R., Arnts, R.R., Guenther, A.: A review and synthesis of monoterpene speciation from forests in the United States. Atmos. Environ. **34**, 1761–1781 (2000)

Gill, K.J., Hites, R.A.: Rate constants for the gas-phase reactions of the hydroxyl radical with isoprene, α- and β-pinene, and limonene as a function of temperature. J. Phys. Chem., A **106**, 2538–2544 (2002)

Holzinger, R., Lee, A., Paw U, K.T., Goldstein, A.H.: Observations of oxidation products above a forest imply biogenic emissions of very reactive compounds. Atmos. Chem. Phys. **5**, 67–75 (2005)

Jaoui, M., Leungsakul, S., Kamens, R.M.: Gas and particle products distribution from the reaction of beta-caryophyllene with ozone. J. Atmos. Chem. **45**, 261–287 (2003)

Joseph, J.H.: Delta-Eddington approximation for radiative flux-transfer. J. Atmos. Sci. **33**, 2452 (1976)

Kaharabata, S.K., Schuepp, P.H., Fuentes, J.D.: Source footprint considerations in the determination of volatile organic compound fluxes from forest canopies. J. Appl. Meteorol. **38**, 878–884 (1999)

Madronich, S.: Photodissociation in the atmosphere.1. actinic flux and the effects of ground reflections and clouds. J. Geophys. Res.-Atmos. **92**(D8), 9740–9752 (1987)

Makar, P.A., Fuentes, J.D., Wang, D., Staebler, R.M., Wiebe, H.A.: Chemical processing of biogenic hydrocarbons within and above a temperate deciduous forest. J. Geophys. Res. **104**, 3581–3603 (1999)

Montzka, S.A., Trainer, M., Goldan, P.D., Kuster, W.C., Fehsenfeld, F.C.: Isoprene and its oxidation products, methyl vinyl ketone and methacrolein, in the rural troposphere. J. Geophys. Res. **98**, 1101–1111 (1993)

Montzka, S.A., Trainer, M., Angevine, W.M., Fehsenfeld, F.C.: Measurements of 3-methyl furan, methyl vinyl ketone, and methacrolein at a rural forested site in the southeastern Unites States. J. Geophys. Res. **100**, 11393–11401 (1995)

Orwig, D.A., Abrams, M.D.: Land-use history (1720–1992), composition, and dynamics of oak pine forests within the piedmont and coastal-plain of northern Virginia. Can. J. For. Res. **24**, 1216–1225 (1994)

Sigler, J.M., Fuentes, J.D., Heitz, R.C., Garstang, M., Fisch, G.: Ozone dynamics and deposition processes at a deforested site in the Amazon Basin. Ambio **31**, 21–27 (2002)

Sillman, S., Carroll, M.A., Thornberry, T., Lamb, B.K., Westberg, H., Brune, W.H., Faloona, I., Tan, D., Shepson, P.B., Sumner, A.L., Hastie, D.R., Mihele, C.M., Apel, E.C., Riemer, D.D., Zika, R.G.: Loss of isoprene and sources of nighttime OH radicals at a rural site in the United States: results from photochemical models. J. Geophys. Res.-Atmos. **107**(D5-6), Art. No. 4043 (2002)

Stockwell, W.R., Kirchner, F., Kuhn, M., Seefeld, S.: A new mechanism for regional atmospheric chemistry modeling. Journal of Geophysical Research **102**, 25847–25879 (1997)

Strong, C., Fuentes, J.D., and Baldocchi, D.: Reactive hydrocarbon flux footprints during canopy senescence. Agric. For. Meteorol. **127**, 159–173 (2004)

Stroud, C., Makar, P., Karl, T., Guenther, A., Geron, C., Turnipseed, A., Nemitz, E., Baker, B., Potosnak, M., Fuentes, J.D.: Role of canopy-scale photochemistry in modifying biogenic-atmosphere exchange of reactive terpene species: Results from the CELTIC field study. J. Geophys. Res.-Atm. **110**(D17), Art. No. D17303 (2005)

Sumner, A.L., Shepson, P.B., Couch, T.L., Thornberry, T., Carroll, M.A., Sillman, S., Pippin, M., Bertman, S., Tan, D., Faloona, I., Brune, W., Young, V., Cooper, O., Moody, J., Stockwell, W.: A study of formaldehyde chemistry above a forest canopy. J. Geophys. Res.-Atmos **106**(D20), 24387–24405 (2001)

Tan, D., Faloona, I., Simpas, J.B., Brune, W., Shepson, P.B., Couch, T.L., Sumner, A.L., Carroll, M.A., Thornberry, T., Apel, E., Riemer, D., Stockwell, W.: HOx budgets in a deciduous forest: Results from the PROPHET summer 1998 campaign. J. Geosphys. Res.-Atmos. **106**(D20), 24407–24427 (2001)

Thornberry, T., Carroll, M.A., Keeler, G.J., Sillman, S., Bertman, S.B., Pippin, M.R., Ostling, K., Grossenbacker, W., Shepson, P.B., Cooper, O.R., Moody, J.L., Stockwell, W.R.: Observations of reactive oxidized nitrogen and speciation of NOy during the PROPHET summer 1998 intensive, J. Geophys. Res.-Atmos. **106**, 24359–24386 (2001)

Wilson, K.B., Baldocchi, D.D., Hanson, P.J.: Leaf age affects the seasonal pattern of photosynthetic capacity and net ecosystem exchange of carbon in a deciduous forest. Plant Cell Environ. **24**, 571–583 (2001)